

STRUCTURE OF FLOW THROUGH AN IMMOVABLE GRANULAR LAYER

U. Dalabaev

UDC 532.529

A solution of the problem of flow through an immovable granular layer is presented.

In view of the fact that filtration of a gas or a liquid in a granular layer provides a basis for various processes of chemical technology, a number of works have been devoted to investigations of the flow structure [1-7]. For example, in [3], the emergence of a strong inhomogeneity of the velocity field behind a granular layer was found experimentally, which was explained by the inhomogeneous stressed state of the layer. In the same work, an analytical solution of the problem of motion of an ideal fluid through a porous medium with a curvilinear boundary within the framework of the model of a "quasi-ideal" fluid was presented. The solution revealed an inhomogeneity in the velocity profile behind the granular layer with the maximum value observed on the wall. In [8], with the use of the electrodiffusion method, velocity profiles were measured not only behind the layer but also in the layer itself. The effect of the shape of the granular layer on the flow structure behind the layer has also been studied. In this case, an inhomogeneous velocity profile behind the layer has been revealed. The description of flow through a granular layer is based on the interpenetration model [9-11]. If one assumes within the framework of a two-velocity model that: 1) the discrete phase is immovable, 2) deformation of the discrete phase can be neglected, 3) heat and mass transfer between the phases does not take place, and 4) the flow is incompressible, then the equations of motion in dimensionless Cartesian coordinates are as follows:

$$\begin{aligned} \varepsilon u_k \frac{\partial u_j}{\partial x_k} = & -\frac{\varepsilon}{\text{Re}} \frac{\partial p}{\partial x_j} + \frac{1}{\text{Re}} \left(\frac{1}{3} \delta_j^k + 1 \right) \frac{\partial}{\partial x_k} \left(\varepsilon \frac{\partial u_j}{\partial x_k} \right) + \\ & + \frac{1}{\text{Re}} \left(1 - \frac{5}{3} \delta_j^k \right) \frac{\partial}{\partial x_k} \left(\varepsilon \frac{\partial u_{3-j}}{\partial x_{3-k}} \right) - \frac{D^2 (1-\varepsilon)^2}{\text{Re} \varepsilon} u_j, \end{aligned} \quad (1)$$

$$\frac{\partial \varepsilon u_k}{\partial x_k} = 0, \quad (2)$$

where $\text{Re} = \rho U h / \mu$ and $D = \sqrt{\alpha} h / d$.

Summation over the index k is assumed in Eqs. (1) and (2). Of the interaction forces [11], Eq. (1) accounts for only the Stokes loss as applied to the flow through a porous layer in Ergun's form [3, 7], with α being the experimentally determined proportionality coefficient (for porous media consisting of spheres, $\alpha \sim 150$). The dimensionless variables are related to the dimensional in the following manner:

$$x_k = \frac{x'_k}{h}, \quad u_i = \frac{u'_i}{U}, \quad p = \frac{\text{Re} p'}{\rho U^2}.$$

It should be noted that if we assume that $\varepsilon \rightarrow 1$ in Eqs. (1)-(2), we arrive at the Navier-Stokes equation. After corresponding simplifications, Eq. (1) transforms into the Darcy equations.

Equations (1) and (2) describe the flow motion not only within the porous layer but also outside it (at $\varepsilon = 1$) and thus make it possible to study conjugate problems outside and within the layer in a uniform manner.

To solve Eqs. (1) and (2) numerically under the corresponding boundary conditions, we used the SIMPLE algorithm developed for the Navier–Stokes equation with the corresponding generalizations [12].

We investigate a flat channel with a granular layer. Let us direct the x_1 axis along the channel axis, and x_2 in the perpendicular direction. A symmetrical velocity profile is preset at the entrance of the channel, which makes it possible to solve the problem only in the upper portion of the channel.

Thus, Eqs. (1)-(2) are considered in the region $0 \leq x_1 \leq L$, $0 \leq x_2 \leq 0.5$.

Let a region of the channel, say $x_{\text{left}} \leq x_1 \leq x_{\text{right}}(x_2)$, $0 \leq x_2 \leq 0.5$, be filled with a granular medium. Now we formulate the boundary conditions. The conditions of flow symmetry

$$x_2 = 0, \quad \frac{\partial u_1}{\partial x_2} = 0, \quad u_2 = 0.$$

are set up on the channel axis. Stick boundary conditions are assumed to be satisfied on the portion of the channel wall which is free of the granular medium, i.e., $x_2 = 0.5$ and $u_1 = u_2 = 0$ for $0 \leq x_1 \leq x_{\text{left}}$, $x_{\text{right}}(0.5) \leq x_1 < L$, and on the boundary which is in contact with the granular medium, i.e., when $x_{\text{left}} \leq x_1 \leq x_{\text{right}}$, we have:

$$x_2 = 0, \quad \frac{\partial u_1}{\partial x_2} = 0, \quad u_2 = 0. \quad (3)$$

It should be noted that assuming a stick boundary condition on the boundary of the porous medium is not quite correct for averaged equations such as Eqs. (1) and (2), since the outer walls do not differ from the inner ones, for which the stick boundary condition is not satisfied. By the same reasoning, a slip boundary condition (3) is assumed for the longitudinal velocity instead of a stick boundary condition.

The following conditions are set up at the entrance of the channel ($0 \leq x_2 \leq 0.5$):

$$x_1 = 0, \quad u_1 = \varphi(x_2), \quad \frac{\partial u_2}{\partial x_1} = 0, \quad p = p_0.$$

At a reasonable distance from the granular medium, a weak condition is set up:

$$x = L, \quad \frac{\partial u_1}{\partial x_1} = \frac{\partial u_2}{\partial x_1} = 0.$$

In simulations, we used an inhomogeneous 40×10 grid and assumed that $L = 3$ and $D = 100$. In the vicinity of the entrance to and exit from the layer we used a finer grid, then nodes obeying the law $h_i = h_{i-1}(1 + \delta)^i$ were used, and nodes with a higher density at the wall were used along the x_2 axis.

We considered several variants of the granular layer layout. The porosity of the granular layer was assumed to be constant and was taken in calculations to equal 0.4.

In order to investigate the effect of the shape of the granular layer, we carried out calculations with three variants of filling of the flat channel: in the first variant the granular layer is situated in the region $0 \leq x_1 < 1$, $0 \leq x_2 \leq 0.5$, in the second variant the right boundary of the granular medium is convex, i.e., has the shape $x_{\text{right}} = 1.06 - 0.24x_2^*$ (i.e., the bend of the right boundary is 6% of the channel size), and in the third variant the right surface is concave, i.e., $x_{\text{right}} = 1 + 0.24x_2^2$. In all the three variants a uniform velocity profile and $\rho_0 = 10^5$ were at the input. Calculations were carried out at $\text{Re} = 1, 10$, and 100. Figure 1a shows longitudinal velocity profiles behind the layer in the cross section $x_1 = 1.07$ ($\text{Re} = 100$); the numbers at the curves correspond to the number of the variant. The considerable effect of the shape of the right boundary of the layer on the velocity distribution behind the layer is evident from the figure. Sharp maxima near the channel walls and the minimum on its axis observed in the second variant appear at all the Reynolds numbers under consideration, and an increase in the value of Re

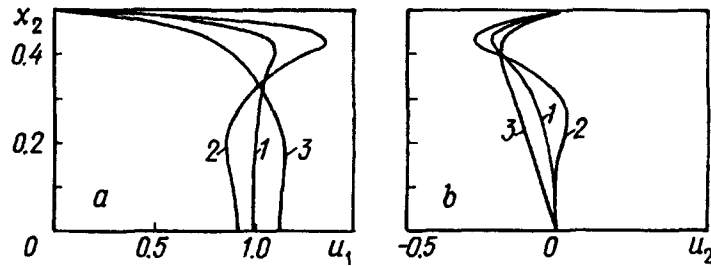


Fig. 1. Changes in longitudinal (a) and transverse (b) velocities for different shapes of the porous layer at the cross section $x_1 = 1.07$, $Re = 100$.

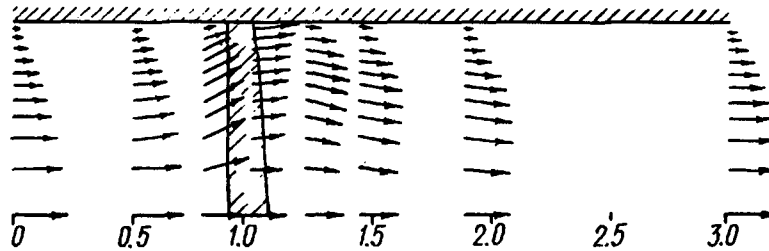


Fig. 2. Evolution of the velocity profile over the entire channel in the case when the channel region $0.9 \leq x_1 \leq 1.03 - 0.12x_2^2$, $0 \leq x_2 \leq 0.5$ is filled with the granular medium ($Re = 10$).

leads to an increase in the ratio $u_{1\max}/u_{1\min}$. Thus, e.g., at $Re = 10$ we have $u_{1\max}/u_{1\min} = 1.46$, and at $Re = 100$ the ratio equals 1.55.

Figure 1b presents changes in the transverse velocity at the cross section $x_1 = 1.07$ at $Re = 100$ for the three variants of the layout of the granular layer, which demonstrates the considerable effect of the shape of the right boundary of the granular layer.

We also investigated the effect of the shape of the granular medium on the flow structure not only behind, but also in front of the layer. To do this, we assumed in the calculations that the granular layer fills the flat channel in the region $0.9 \leq x_1 \leq x_{\text{right}}(x_2)$. At the entrance of the channel we set up a parabolic distribution law of the longitudinal velocity. In this case we observed exactly the same pattern behind the layer as in the three above-considered variants of the shape of the right boundary of the porous region. Inhomogeneity of the velocity profile is observed not only behind, but also in front of the layer.

Figure 2 presents the evolution of the velocity profile over the entire channel and several cross sections in the case when the right boundary of the layer is $x_{\text{right}}(x_2) = 1.03 - 0.12x_2^2$. The velocity maximum in the vicinity of the wall is observed not only behind the layer, but also in the layer itself.

Thus, the geometrical shape of the exit boundary of a porous medium affects substantially the flow structure; it is one of the main reasons for the emergence of "ears" in the boundary region not only behind, but also in front of the layer. In this case the maximum value of the longitudinal velocity behind the layer takes place in the vicinity of the wall, and not on the wall itself, as in [3]. It should be noted that the revealed emergence of the "ears" is similar to experimental data [8], which results from taking into account viscosity terms in equations of motion.

NOTATION

x_1, x_2 , dimensionless Cartesian coordinates; x'_1, x'_2 , dimensional coordinates; u_1, u_2 , dimensionless velocities; u'_1, u'_2 , dimensional coordinates; p, p' , dimensionless and dimensional pressures; ρ , flow density; U , volume-averaged velocity; h , channel width; d , characteristic size of granular medium; Re , Reynolds number; ε , porosity of granular medium; D , dimensionless number; α , proportionality coefficient; L , dimensionless channel length; $x_{\text{left}}, x_{\text{right}}$, left and right boundaries of granular medium (dimensionless); $u_{1\min}, u_{1\max}$, minimum and maximum values of the dimensionless longitudinal velocity over the cross section; h_i , grid spacing.

REFERENCES

1. M. É. Aérov, O. M. Todes, and D. A. Narinskii, Apparatuses with a Stationary Granular Layer. Hydraulic and Thermal Principles of Operation [in Russian], Leningrad (1979).
2. N. P. Tabunshchikov, Zh. Prikl. Khim., 29, Issue 1, 32-40 (1956).
3. M. A. Gol'dshtik, Transfer Processes in a Granular Layer [in Russian], Novosibirsk (1984).
4. E. K. Popov, E. V. Smirnova, G. N. Ataeva, P. G. Shtern, S. V. Turuntaev, and V. F. Lychkin, in: Aerodynamics of Chemical Reactors [in Russian], Novosibirsk (1976), pp. 65-68.
5. Dao-Min'-Ngok, Vestnik MGU, Ser. 1, No. 5, 74-78 (1980).
6. I. V. Shirko, in: Numerical Simulation in Aerohydrodynamics [in Russian], Moscow (1986), pp. 236-246.
7. V. P. Myasnikov and V. D. Kotelkin, in: Aeromechanics [in Russian], Moscow (1976), pp. 307-316.
8. V. A. Kirillov, V. A. Kuz'min, V. I. P'yanov, and V. M. Khanaev, Dokl. Akad. Nauk SSSR, 245, No. 1, 159-162 (1979).
9. Kh. A. Rakhmatulin, Prikl. Math. Mekh., No. 2, 184-190 (1956).
10. D. F. Faizullaev, Laminar Motion of Multiphase Media in Pipelines [in Russian], Tashkent (1966).
11. R. I. Nigmatullin, Principles of Mechanics of Heterogeneous Media [in Russian], Moscow (1978).
12. S. Patankar, Numerical Methods of Solving Problems of Heat Transfer and Dynamics of Fluids [Russian translation], Moscow (1984).